Scientific Journal of Silesian University of Technology. Series Transport
Zeszyty Naukowe Politechniki Śląskiej. Seria Transport

Volume 131 **2026**

p-ISSN: 0209-3324

e-ISSN: 2450-1549

DOI: https://doi.org/10.20858/sjsutst.2026.131.11

Journal homepage: http://sjsutst.polsl.pl

Article citation information:
Protsenko, V., Rusanov, S., Babiy, M., Kliuiev, O., Voitovych, O. Analysis of water transfer centrifugal pump shaft dynamic loads under different operating modes. *Scientific Journal of Silesian University of Technology. Series Transport*. 2026, **131**, 177-188. ISSN: 0209-3324. DOI: https://doi.org/10.20858/sjsutst.2026.131.11

Vladyslav PROTSENKO[1], Sergiy RUSANOV[2], Mykhailo BABIY[3], Oleg KLIUIEV[4], Olha VOITOVYCH[5]

ANALYSIS OF WATER TRANSFER CENTRIFUGAL PUMP SHAFT DYNAMIC LOADS UNDER DIFFERENT OPERATING MODES

Summary. The article addresses the dynamics of an water transfer centrifugal pump drive with a asynchronous electric motor operating on a filled reservoir. A three-mass dynamic model of the drive has been developed, and the equations of motion for the masses have been formulated. Friction losses inside the pump, pipeline resistance, and the inertial resistance of the fluid in the pipeline have been taken into account. The torque of the asynchronous drive motor is described by the Kloss equation. The numerical solution of the dynamic equations shows that the most dangerous scenario in terms of the strength of the pump's main shaft and motor overheating is startup with the delivery valve open, as overload here approaches approximately 20 times the nominal value. It has been established that during pump startup with the delivery valve closed, shaft overload can reach 160%, while sudden

[1] Faculty of Engineering and Transport, Kherson National Technical University, Institutska st., 11, 29016, Khmelnitsky, Ukraine. Email: 1904pvo@gmail.com. ORCID: https://orcid.org/0000-0002-3468-4952
[2] Faculty of Engineering and Transport, Kherson National Technical University, Institutska st., 11, 29016, Khmelnitsky. Email: ohvpbm@i.ua. ORCID: https://orcid.org/0000-0002-1003-4867
[3] Faculty of Marine Energetics, Kherson State Maritime Academy, Kanatna st., 99, 65012, Odesa. Ukraine. Email: m_babiy@ukr.net. ORCID: https://orcid.org/0000-0002-0560-2081
[4] Faculty of Engineering and Transport, Kherson National Technical University, Institutska st., 11, 29016, Khmelnitsky. Email: kluevoi@ukr.net. ORCID: https://orcid.org/0000-0001-6803-0706
[5] Faculty of Engineering and Transport, Faculty of Engineering and Transport, Kherson National Technical University, Institutska st., 11, 29016, Khmelnitsky, Ukraine. Email: olgavoytovich@ukr.net. ORCID: https://orcid.org/0000-0003-0510-4362

opening of the valve on the delivery pipeline results in 180%. It is shown that transient operating modes of the pump drive are accompanied by intense torsional vibrations, which reduce shaft service life and must be considered in refined calculations. The cases examined are of practical value, as they underscore the need to follow pump operating procedures.

Keywords: centrifugal pump, shaft, dynamic load, torque, oscillations, failure, operation

1. INTRODUCTION

Centrifugal pumps are among the most common devices in transport systems, including pipelines and marine vessels, where they perform critical functions in ballast systems, cooling systems of power units, and cargo systems of tankers. To ensure reliable operation of pumps - particularly their most stressed components, such as shafts - it is necessary to reduce dynamic loads in their drives. This can be achieved by adhering to established maintenance and operational requirements. Operators and engineering students often fail to realize how violations of operating rules affect the performance and wear of components. This forms the basis for studying the operational conditions influencing the service life of centrifugal pump shafts.

Fig. 1. Photograph of the fatigue fracture surface of the shaft (stress concentrator – thread) [1]

Fig. 2. Photograph of the fatigue fracture surface of the pump shaft (stress concentrator – keyway) [3]

The most expensive and frequently damaged components of centrifugal pumps are the main shafts, on which the impeller and semi coupling of the motor coupling are mounted. Replacing a shaft requires nearly complete disassembly of the pump, removal of the impeller and bearings, resulting in equipment downtime and considerable human and material resource costs.

Study [1] investigated the failure of a centrifugal pump shaft after many operating cycles. Using chemical analysis, microstructural analysis, and fractography, and employing the modified Goodman criterion to evaluate fatigue stress, it was determined that a fatigue crack initiated in the area of an existing stress concentrator - the thread (Fig. 1). The study also noted insufficient fatigue strength under fluctuating loads and recommended revising the thread geometry while accounting for variable stresses. Study [2] analyzed shaft failure in a pump at a steel plant after 2.5 years of operation near the keyway. Metallography, mechanical testing, and geometric analysis of the keyway were employed. It was found that even small deviations in keyway geometry can cause stress concentration and fatigue crack initiation. The shaft material exhibited insufficient heat-treatment quality, reducing fatigue strength and leading to crack initiation and propagation under dynamic loading. Study [3] described the failure of a circulation pump shaft in a chemical plant cooling system. Using chemical and structural analysis and fractography, it was shown that calcium-silicate inclusions on the shaft surface served as crack initiators, which under cyclic dynamic loads resulted in fatigue fracture. Improved material cleanliness and heat treatment were recommended. Study [4] analyzed the failure of a condensate pump shaft at a thermal power station after 5 years of operation. Visual inspection, microstructural and chemical analysis, and fractography indicated that the failure was caused by stress concentration and sulfide inclusions near the surface, leading to fatigue failure due to torsional vibrations. Study [5] discussed the failure of slurry transport pump shafts. Using chemical analysis, metallography, and mechanical testing, it was found that improper heat treatment regimens caused reduced fatigue strength and premature shaft failure. Similar results were obtained in [6], where poor repair quality caused shaft failure two days after reassembly. Paper [7] described six cases of shaft failure in cooling water pumps on a container vessel and analyzed the two most recent ones. It was established that shafts failed due to fatigue caused by dynamic loads at stress concentrators (keyways) and improper material selection. Stress concentrators also caused shaft failure in a multistage centrifugal pump [8], where it was shown that reducing stress concentration through design modifications can increase shaft life under torsional vibration. Modeling of a three-stage centrifugal water pump under variable load was carried out in [9]. The study focused on the effect of hydrodynamic forces on shaft fatigue stress and demonstrated that conventional calculations underestimate dynamic loads. Regions of hydrodynamic pressure concentration and cyclic loading were identified. The proposed approach was recommended for pump shaft design under variable load. The fatigue failure of a hydraulic coke-removal system pump shaft at a metallurgical plant was reported in [10]. Metallography, chemical analysis, and fractography confirmed that cracks developed due to cyclic torsional loading. Fatigue failure of a thermal power station circulation water pump shaft was analyzed in [11]. Material porosity was found to be the main cause of fatigue fracture. Study [12] described fatigue failure of a centrifugal pump shaft in a diesel engine cooling system, where the initial crack formed at a stress concentrator under torsional vibrations. The study recommended accurate stress evaluation in design calculations. Paper [13] described premature failure of an electric submersible pump shaft in an oil field and recommended reducing shaft overload. Research [14] summarized statistical data from 2015 to 2024 on pump failures in the oil, gas, chemical, and water supply industries in Ukraine. It was found that 78% of failures involved mechanical damage, 15% hydraulic, 5% electrical, and 2% corrosion-related causes.

Summarizing the review, it can be stated that regardless of the origin of fatigue cracks - foreign inclusions, porosity, stress concentrators, or machining and heat-treatment defects - the cause of crack formation lies in dynamic loads in the pump drive, which induce shaft vibrations.

To perform refined dynamic calculations, it is necessary to derive and solve the equations of motion for the pump drive components under external torque disturbances from both the motor driving and hydraulic resistance. Studies on the dynamics of centrifugal pump drives are scarce; only [15] examines natural oscillations of vertical pump drive components.

Thus, the purpose of this study is to analyze the dynamics of a centrifugal pump drive under various operational conditions.

Tasks of the study:

- to develop a dynamic model of a centrifugal pump drive and derive equations of motion for its masses;
- to formulate the disturbance torque equations for both driving and resisting moments;

- to describe the main operational cases and specify initial conditions for the equations of motion;
- to select a specific pump system for analysis and determine constant parameters;
- to analyze dynamic loads on the pump shaft by solving the derived system for characteristic operating cases;
- to rank the cases in terms of their hazard to the static and fatigue strength of the pump shaft.

2. METHODOLOGY

The schematic of the model pump system is shown in Fig. 3. It includes a suction pipeline with inlet filter 1 and suction valve 2, through which the centrifugal pump 3 draws fresh water. The discharge pipeline has a pressure valve 4 and a check valve 5 preventing fluid backflow from tank 6. The pump 3 is driven by an asynchronous motor 8 via an elastic coupling 7.

When developing and analyzing the dynamic model, materials from studies describing basic modeling principles [16], mass and force reduction [17], and examples of dynamic analysis [18] were used. The asynchronous motor characteristics can be approximated using the Kloss formula [20], despite the underlying complexity of electromagnetic interactions [19]. Inside a centrifugal pump, there are quite complex transient processes associated with the unsteady rotation of the fluid [21], here we use well-known materials [22] for internal losses in pump housing. Pipeline losses we definite according to standard hydromechanics [23, 24].

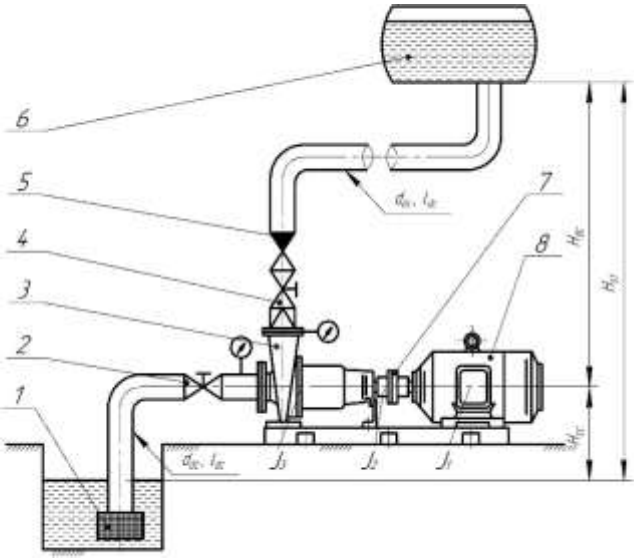

Fig. 3. Schematic diagram of a pump unit with centrifugal pump and induction motor

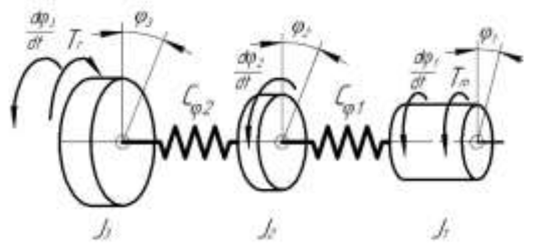

Fig. 4. Three-mass torsional dynamic model of the pump driving

The dynamic model of the pump unit is represented as a three-mass system (Fig. 4), where the driven mass J_3 is formed by the pump impeller, the intermediate mass J_2 by the driven semicoupling of the flexible coupling, and the driving mass J_1 by the electric motor rotor and the driving semicoupling of the same coupling.

The masses are connected by elastic elements - a shaft with torsional stiffness $C_{\varphi 2}$ and a flexible coupling with torsional stiffness $C_{\varphi 1}$.

When developing the dynamic model, the following assumptions were made:
- the pipelines are considered perfectly rigid;
- the elastic elements of the couplings have constant stiffness and zero damping;
- the hydraulic resistance coefficients in the pipeline and inside the pump do not depend on the fluid velocity.

The system of motion equations for such a system will be [12-14]:

$$\begin{cases} J_1 \cdot \dfrac{d^2\varphi_1}{dt^2} + C_{\varphi 1} \cdot (\varphi_1 - \varphi_2) = T_m; \\ J_2 \cdot \dfrac{d^2\varphi_2}{dt^2} + C_{\varphi 2} \cdot (\varphi_2 - \varphi_3) = C_{\varphi 1} \cdot (\varphi_1 - \varphi_2); \\ J_3 \cdot \dfrac{d^2\varphi_3}{dt^2} + T_r = C_{\varphi 2} \cdot (\varphi_2 - \varphi_3), \end{cases} \tag{1}$$

where φ_1, φ_2 and φ_3 are the angular coordinates of the respective masses; T_m is the electric motor torque; T_{tr} is the resistance torque.

The torque of the asynchronous electric motor by Kloss equation [20]:

$$T_m = 2T_{cr} \frac{(\omega_s - \omega_{cr}) \cdot \left[\omega_s - \dfrac{d\varphi_1}{dt} \right]}{(\omega_s - \omega_{cr})^2 + \left[\omega_s - \dfrac{d\varphi_1}{dt} \right]^2} = \frac{A \cdot \left[\omega_s - \dfrac{d\varphi_1}{dt} \right]}{B + \left[\omega_s - \dfrac{d\varphi_1}{dt} \right]^2}, \tag{2}$$

where T_{cr} is the critical torque; ω_s is the synchronous rotor rotation frequency; ω_{cr} is the critical rotor rotation frequency.

The resistance torque T_r reduced to the impeller include disk friction torque in the pump T_{df} and load from the pipeline T_{tb}:

$$T_r = T_{df} + T_{tb}. \tag{3}$$

Disc friction torque will be [17, 18]:

$$T_{df} = (2{,}4 \ldots 2{,}7) c_f \rho R^5 \omega^2 = \chi \omega^2 = \chi \left(\frac{d\varphi_3}{dt} \right)^2, \tag{4}$$

where 2,4…2,7 is a coefficient that accounts for losses from both impeller ends, increased friction in a real pump compared to a model disk, and friction losses in the seal; $c_f = 0{,}0465 Re^{-0{,}2}$ is the friction coefficient depending on the fluid flow regime inside the pump and the magnitude of the ratio of the gap between the impeller ends and the housing (*Re* is the Reynolds criterion); *R* is the impeller radius.

The load acting on the pump impeller from the pipeline side consists of the torque T_{st} due to the static head of the pipeline, the torque T_{tr} caused by the hydraulic resistance in the pipeline, and the torque T_{in} resulting from the inertia of the liquid in the filled pipe:

$$T_{tb} = T_{st} + T_{tr} + T_{in}. \tag{5}$$

Torque T_{st} from static head H_{st} will be:

$$T_{st} = \rho g H_{st} \frac{Q}{\omega} = \alpha \cdot \frac{Q}{\frac{d\varphi_3}{dt}} \tag{6}$$

The torque from hydraulic resistance in the pipeline reduced to pump impeller J_3 [19]:

$$T_{tr} = \rho g H_{fr} \frac{Q}{\omega} = \frac{8\rho}{\pi^2} \cdot \left\{ \frac{1}{d_{sc}^4} \left[\lambda \frac{l_{sc}}{d_{sc}} + \sum \xi_{sc} \right] + \frac{1}{d_{dc}^4} \left[\lambda \frac{l_{dc}}{d_{dc}} + \sum \xi_{dc} \right] \right\} \cdot \frac{Q^3}{\omega} = \beta \cdot \frac{Q^3}{\frac{d\varphi_3}{dt}}, \tag{7}$$

where d_{sc} is the suction pipeline diameter; d_{ds} is the discharge pipeline diameter; l_{sc} is the suction pipeline length; l_{ds} is the discharge pipeline length; ξ are local resistance coefficients (valves, filters); λ is the Darcy coefficient.

For torque T_{in} from static inertial head H_{in} we will have:

$$T_{in} = \rho g H_{in} \frac{Q}{\omega} = \frac{4\rho}{\pi} \cdot \left(\frac{l_{sc}}{d_{sc}^2} + \frac{l_{dc}}{d_{dc}^2} \right) \cdot \frac{Q}{\omega} \cdot Q' = \gamma \cdot \frac{Q}{\frac{d\varphi_3}{dt}} \cdot \frac{dQ}{dt}. \tag{8}$$

Taking into account pump efficiency value η = 0,8, we will get expression for pipeline resistance torque, reduced to pump impeller J_3:

$$T_r = \chi \omega^2 + \frac{1}{\eta} \cdot \left(\alpha \cdot \frac{Q}{\omega} + \beta \cdot \frac{Q^3}{\omega} + \gamma \frac{Q}{\omega} Q' \right) = \chi \left(\frac{d\varphi_3}{dt} \right)^2 + \frac{1{,}25Q}{\frac{d\varphi_3}{dt}} \cdot \left(\alpha + \beta \cdot Q^2 + \gamma \cdot \frac{dQ}{dt} \right). \tag{9}$$

Taking into account the recorded disturbing torques, the resulting dynamic model can be expressed by the following system of equations (10).

$$\begin{cases} J_1 \cdot \dfrac{d^2\varphi_1}{dt^2} + C_{\varphi 1} \cdot (\varphi_1 - \varphi_2) = \dfrac{A \cdot \left[\omega_s - \dfrac{d\varphi_1}{dt} \right]}{B + \left[\omega_s - \dfrac{d\varphi_1}{dt} \right]^2}; \\ J_2 \cdot \dfrac{d^2\varphi_2}{dt^2} + C_{\varphi 2} \cdot (\varphi_2 - \varphi_3) = C_{\varphi 1} \cdot (\varphi_1 - \varphi_2); \\ J_3 \cdot \dfrac{d^2\varphi_3}{dt^2} + + \chi \cdot \left(\dfrac{d\varphi_3}{dt} \right)^2 + \dfrac{1{,}25Q}{\frac{d\varphi_3}{dt}} \cdot \left(\alpha + \beta \cdot Q^2 + \gamma \cdot \dfrac{dQ}{dt} \right) = C_{\varphi 2} \cdot (\varphi_2 - \varphi_3). \end{cases} \tag{10}$$

The highest loads on the pump shaft may occur under the following operation conditions:
- starting the pump motor without load when the discharge valve is closed (initial conditions: at $t = 0$; $\varphi_1 = \varphi_2 = \varphi_3 = 0$; $\frac{d\varphi_1}{dt} = \frac{d\varphi_2}{dt} = \frac{d\varphi_3}{dt} = 0$; $Q = 0$);
- opening the discharge valve of the pump while the motor is running (initial conditions: at $t = 0$; $\varphi_1 = 0$; $\varphi_2 = -\frac{T_{df}}{C_{\varphi 1}} = -\frac{\chi\omega_0^2}{C_{\varphi 1}}$; $\varphi_3 = -\frac{T_{df}}{C_{\varphi 1}} - \frac{T_{df}}{C_{\varphi 2}} = -\frac{\chi\omega_0^2}{C_{\varphi 1}} - \frac{\chi\omega_0^2}{C_{\varphi 2}}$; $\frac{d\varphi_1}{dt} = \frac{d\varphi_2}{dt} = \frac{d\varphi_3}{dt} = \omega_0$. The steady-state angular velocity ω_0 of the system before opening the discharge valve is determined by solving system (10) at $Q = 0$);
- starting the pump motor with the opened discharge valve (a mode prohibited by operating regulations but possible in practice; initial conditions: at $t = 0$; $\varphi_1 = \varphi_2 = \varphi_3 = 0$; $\frac{d\varphi_1}{dt} = \frac{d\varphi_2}{dt} = \frac{d\varphi_3}{dt} = 0$).

When opening the discharge valve on a running pump, according to the electrical *RC* analogy, the change in flow rate *Q* is calculated using expression (11) [20].

When starting the pump with the discharge valve open, *Q* is determined using expression (12) [19].

$$Q(t) = Q_n \cdot (1 - e^{-\frac{t}{\tau}}); \tag{11}$$

$$Q(t) = \frac{Q_n}{\omega_n} \cdot \frac{d\varphi_3}{dt} = \psi \cdot \frac{d\varphi_3}{dt}, \tag{12}$$

where ω_n is the nominal angular velocity of the motor; τ is the relaxation time of dynamic processes in the pipeline.

Calculations were performed using the example of a pump unit that includes a centrifugal pump with capacity $Q_n = 400$ $m^3/h = 0.1111$ m^3/s, driven by an asynchronous motor $P = 90$ *kW* at $n_n = 1440$ *rpm* through a flexible pin-bush coupling. The pump operates on a pipeline with diameters $d_{sc} = 0.20$ *m* and $d_{dc} = 0.15$ *m*, length $l_{sc} = 20$ *m*, $l_{dc} = 45$ *m*, transferring fresh water ($\rho = 1000$ kg/m^3) through a filter to a tank at height $H_{st} = 20$ *m* from the water free surface. The pump impeller has mass $m = 42$ *kg* and radius $R = 0.203$ *m*.

For the described pump unit, the constants used will have next values: $T_{cr} = 1373{,}00$ $N \cdot m$, $\omega_n = 150{,}80$ rad/s, $\omega_{cr} = 129{,}60$ rad/s, $\omega_s = 157{,}10$ rad/s, $A = 75410{,}0$ W, $B = 754{,}3$ rad^2/s^2, $\alpha = 196200$ *Pa*, $\beta = 30978014$ $Pa \cdot s^2/m^2$, $\gamma = 3183099$ kg/m^4, $Re = 7\times10^6$, $c_f = 0{,}002$, $\chi = 0{,}0019$ $N \cdot m$ s^2/rad^2, $\psi = 0{,}00072$ m^3/rad, $\tau = 0{,}05$ *s*. The moments of inertia of masses and torsional stiffnesses will be: $J_1 = 0{,}55$ $kg \cdot m^2$, $J_2 = 0{,}15$ $kg \cdot m^2$, $J_3 = 0{,}87$ $kg \cdot m^2$, $C_{\varphi 1} = 80000$ $N \cdot m/rad$, $C_{\varphi 2} = 166154$ $N \cdot m/rad$.

The results of solving the system of equations (10) for the described operating conditions are presented as graphs of the flow rate $Q(t)$, the angular velocities $\frac{d\varphi_i}{dt} = f(t)$ of the corresponding masses, the motor torque $T_m = f(t)$, and the shaft torque $T_{sh} = C_{\varphi 2} \cdot (\varphi_2 - \varphi_3) = f(t)$.

3. RESULTS AND DISCUSSION

Fig. 5…Fig. 7 show the respective plots obtained from the numerical solution of system (10).

Analysis of the graphs in Fig. 5 indicates that the pump acceleration without load occurs in approximately 0.35 s, during which the motor develops sufficient torque T_m to overcome the disc friction torque T_{df}, and the system reaches a steady angular velocity of ω_0 = 156.6 rad/s. The shaft overload during such a startup is characterized by the dynamic factor, defined as the ratio of the maximum torque T_{max} to the nominal torque T_n: $K_d = T_{max}/T_n = 2.60$, where the nominal torque is $T_n = 590\ N{\cdot}m$.

When the discharge valve is opened on a running pump (Fig. 6), the transient process will last approximately 0.3 s, with shaft overload reaching 180%, corresponding to a maximum torque in the shaft of 1650 N·m. The angular velocities of the rotating masses decrease from ω_0 = 156.6 rad/s to approximately ω = 122 rad/s upon valve opening, followed by a return to the nominal angular velocity ω_n = 150.8 rad/s.

The most dangerous scenario is starting the pump with the opened discharge valve (Fig. 7). Here, the system exhibits classic positive feedback behavior until the critical angular velocity is reached (approximately at 0.85 s), which accounts for the significant danger of starting in this configuration. The frequency of the growing oscillations depends on the system's natural frequency, the moment of inertia of the rotating masses, and the slope of the engine's starting characteristic curve. In this case, shaft overload reaches 1800%, which is clearly dangerous for its structural integrity and may lead to plastic deformation. This is naturally accompanied by engine overload, with potential overheating due to the acceleration time being extended fourfold to 1.35 s.

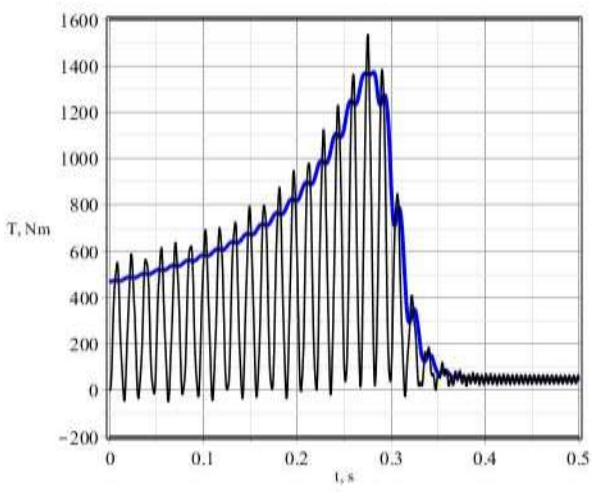

a)

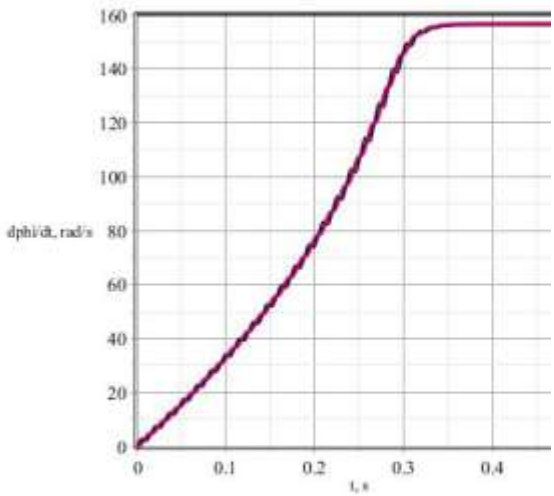

b)

Fig. 5. Graphs of torque variations (a): motor torque (blue) and shaft torque (black), as well as angular velocity variations (b) of the motor rotor (black), driven semicoupling (blue), and pump impeller (red) during no-load pump startup

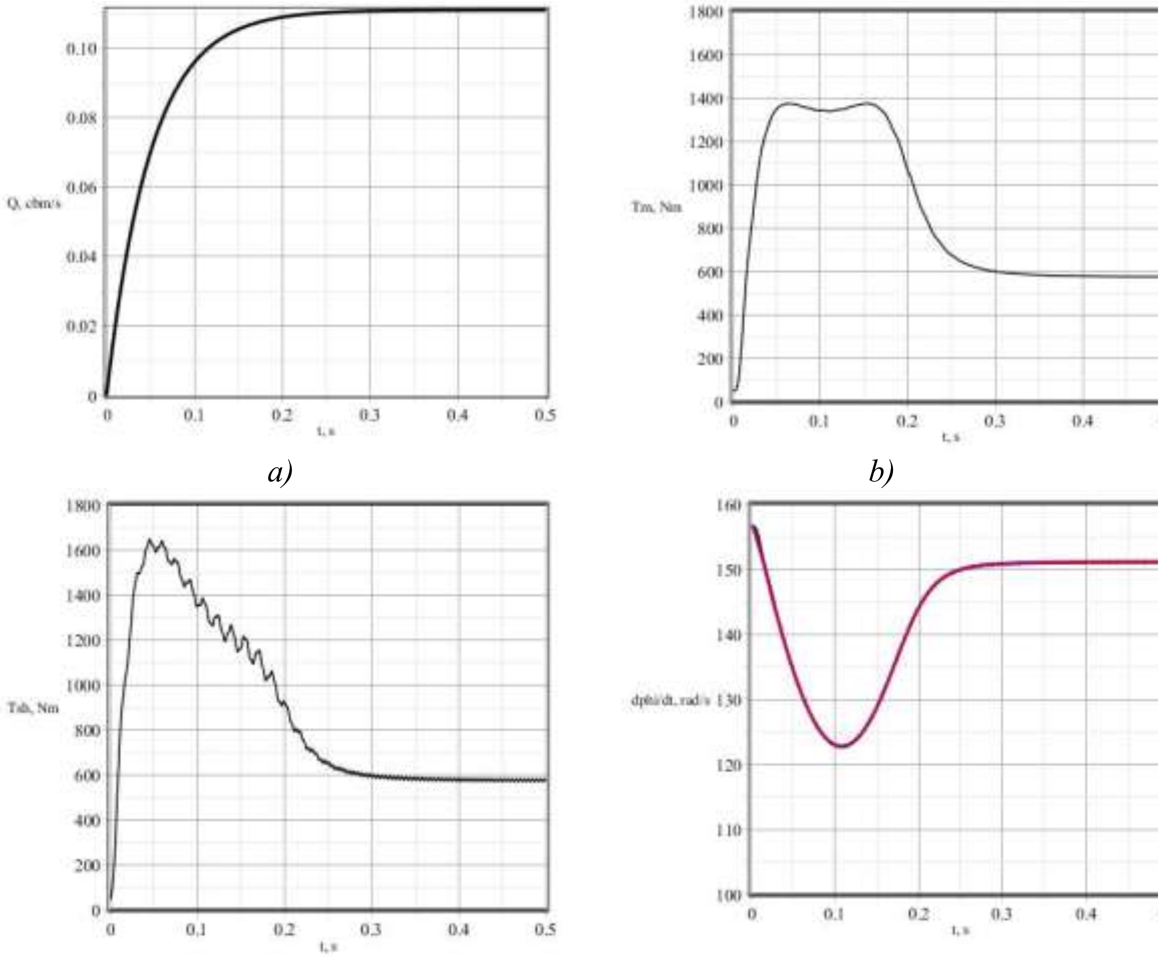

a) b)

c) d)

Fig. 6. Graphs of changes in flow rate (a), engine torque (b) and shaft torque (c), as well as angular velocities (d) of the engine rotor (black), driven semi coupling (blue), and pump impeller (red) when opening the discharge valve on a running pump

4. CONCLUSION

1) The dynamic behavior of a centrifugal pump with an induction drive motor operating under flooded suction conditions has been analyzed. A three-mass dynamic model of the drive was developed, and the equations of motion for the masses and disturbing torques were formulated. The equations were solved for three characteristic cases: pump startup with a closed discharge valve, valve opening during operation, and pump startup with an opened valve.
2) It has been shown that the most critical condition, in terms of the pump main shaft strength and motor overheating, is startup with the discharge valve opened. Under this condition, the shaft dynamic factor may reach K_d = 19, and the startup duration increases nearly fourfold compared to startup with a closed discharge pipeline. This behavior is evidently influenced by the presence of liquid-filled piping, which imposes additional inertial loading.

3) During startup with the discharge valve closed, the shaft dynamic factor may reach K_d =2.60, and when the discharge valve is opened during operation, K_d =2.80. These values correspond to the minimum safety factor that should be incorporated in the strength design of the pump drive.
4) In all analyzed cases, the transient operation modes of the pump drive are accompanied by high-frequency torsional oscillations, which reduce the service life of couplings and shafts. These effects should be accounted for in refined dynamic calculations.
5) The analyzed cases have practical value as illustrative didactic materials demonstrating actual pump operation rules and can be used in the training of maintenance engineers. Another important application is the use of the formulated motion equations for analyzing transient modes in the design of centrifugal pump drives, particularly for identifying methods to reduce dynamic loads in their drivetrains.

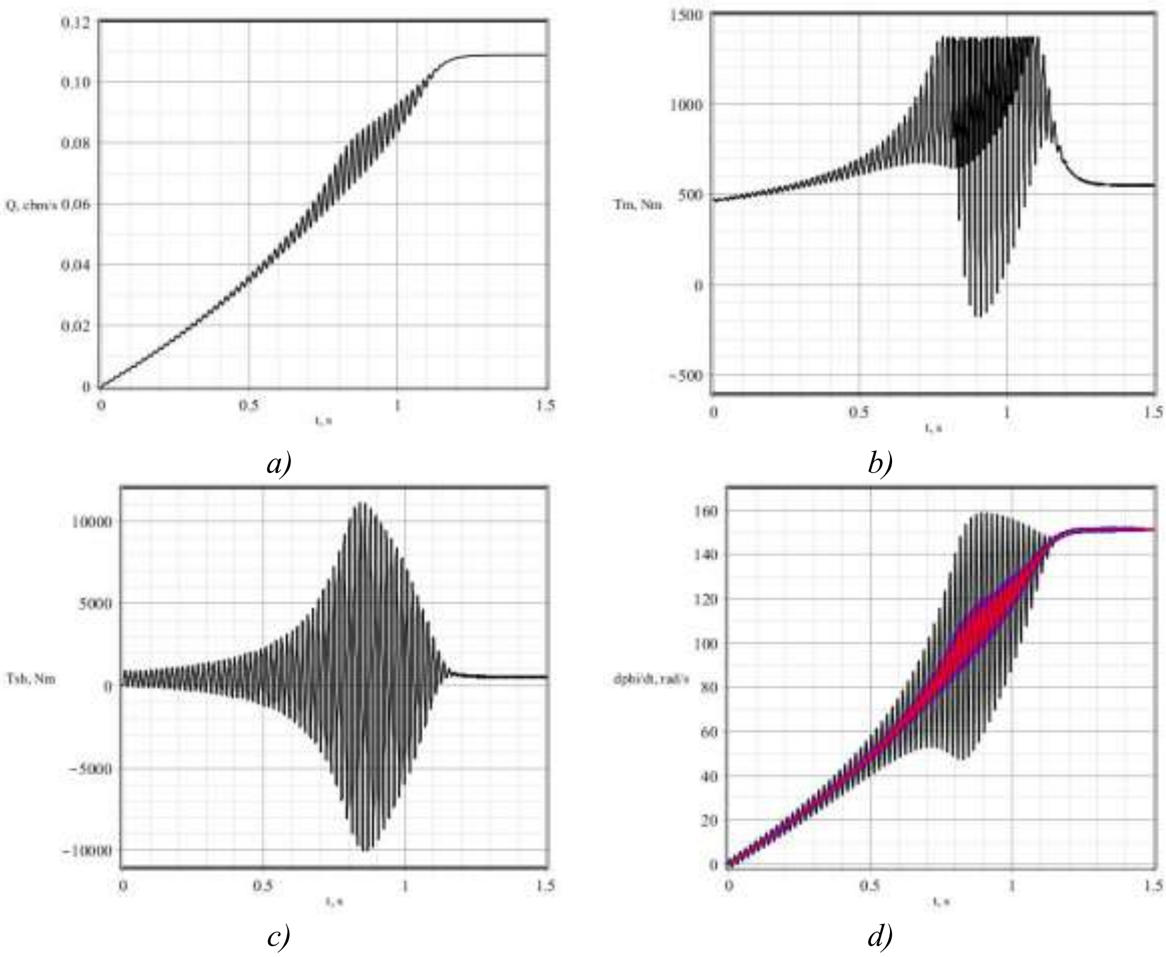

Fig. 7. Graphs of changes in flow rate (a), engine torque (b) and shaft torque (c), as well as angular velocities (d) of the engine rotor (black), driven semi coupling (blue), and pump impeller (red) during pump startup with the discharge valve open

References

1. Tamin M., M.A. Hamzah. 2017. "Fatigue Failure Analysis of a Centrifugal Pump Shaft". In: *Failure Analysis and Prevention. InTech*: 2-15. DOI: 10.5772/intechopen.70672.
2. Roy A., P. Palit, S. Das, G. Mukhyopadyay. 2020. „Investigation of Torsional Fatigue Failure of a Centrifugal Pump Shaft". *Engineering Failure Analysis* 112. No 104511. DOI: 10.1016/j.engfailanal.2020.104511.
3. Jiang C., K. Tao, J. Wang, W. Wang. 2020. „Fracture Failure Analysis of the Pump Shaft". *E3S Web Conf.* 213. No 03010. DOI: 10.1051/e3sconf/202021303010.
4. Ghanem M. 2018. „Failure Analysis of Condensate Pump Shaft in Power Plant". *Key Engineering Materials* 786: 314-318. DOI: 10.4028/www.scientific.net/KEM.786.314.
5. Das G., A.N. Sinha, S.K. Mishra, D.K. Bhattacharya. 1999. „Failure Analysis of Counter Shafts of a Centrifugal Pump". *Engineering Failure Analysis* 6(4): 267-276. DOI: 10.1016/S1350-6307(98)00037-5.
6. Gejdoš P., L. Klakurková, M. Juliš. 2020. „Metallographic Analysis of Stainless Steel Inner Shaft of Centrifugal Pump". *Defect and Diffusion Forum* 405: 223-228. DOI: 10.4028/www.scientific.net/DDF.405.223.
7. Papageorgiou D.G., K. Kovsenoglou, P. Bournelis, C. Medrea. 2018. „Fracture Analysis of a Cooling Water Pump Shaft". *MATEC Web of Conferences* 188. No 04022. DOI: 10.1051/matecconf/201818804022.
8. Hua M., C. Cao, Y. Cai, J. Ge, F. Zhong, J. Mao. 2023. „Failure Analysis and Structural Fatigue Resistance Design of Multistage Centrifugal Pump Shaft". *Engineering Failure Analysis* 153. No 107545. DOI: 10.1016/j.engfailanal.2023.107545.
9. Yadeta L., H.G. Lemu, A.K. Tadese. 2025. „Fluid Structure Interaction Induced Fatigue Stress Analysis of Multi-Stage Centrifugal Water Pump Shaft Under Varying Load Condition". *J Braz. Soc. Mech. Sci. Eng.* 47. No 395. DOI: 10.1007/s40430-025-05703-w.
10. Zhai J.-m., X. Shang, L. Kong. 2021. „Fatigue Failure Analysis of Pump Shaft of a Hydraulic Coke Removal System". *J. Fail. Anal. and Preven.* 21: 861-869. DOI: 10.1007/s11668-021-01124-8.
11. Hamid A., S. Nugroho, G. Dwi, H. Khaeroman. 2018. „Failure Analysis of Shaft Circulating Water Pump (CWP) Used in Power Plant". *MATEC Web of Conferences* 159. No 02027. DOI: 10.1051/matecconf/201815902027.
12. Saiful W., H. Husaini, A. Nurdin. 2021. „Failure Analysis on the Fracture Shaft of a Centrifugal Pump Used for Diesel Engine Cooling System". *Key Engineering Materials* 892: 107-114. DOI: 10.4028/www.scientific.net/KEM.892.107.
13. Pratiwi D., Y. Yudianto, A. Mataram, A. Prakoso. 2023. „Shaft Premature Failure Analysis in Electrical Submersible Pump System: Case Study from Muara Enim, South Sumatra, Indonesia". *Journal of Mechanical Science and Engineering* 9(1).: 7-13. DOI: 10.36706/jmse.v9i1.71.
14. Morshch I.V. 2025. „Analysis of the Causes of Damage to Centrifugal Pumps During Operation and Methods of Their Elimination". *Problems of Tribology* 115: 60-65. DOI: 10.31891/2079-1372-2025-115-1-60-65.
15. Chandra H., M. Luthfi, F. Lamin, A. Ariffin. 2018. „Evaluation of Torsional Vibration on Vertical-Type Centrifugal Pump Shaft". *Journal of Mechanical Engineering* 7(1): 167-175. Available at: https://ir.uitm.edu.my/id/eprint/41508/1/41508.pdf
16. Komarov M.S. 1969. *Dynamics of Mechanisms and Machines*. Moscow: Mashinostroenie.

17. Loveikin V.S., Romasevych Yu.O. 2013. *Dynamics of Machines*. Kyiv: CP „KOMPRINT".
18. Kolesnyk N.P. 1985. *Calculations of Construction Cranes*. Kyiv: Vyshcha Shkola.
19. Klyuchev V.I. 1971. *Limitation of Dynamic Loads of Electric Drive*. Moscow: Energiya.
20. Koljčević N., Ž. Fuštić, M. Ćalasan 2020. „Analytical Solution for Determination of Induction Machine Acceleration Based on Kloss Equation". *Serbian Journal of Electrical Engineering* 17: 247-256. DOI: 10.2298/SJEE2002247K.
21. Ivchenko V. 2019. „On the unsteady rotating fluid flow in a uniformly rotating or fixed vertical cylinder". *European Journal of Physics* 41(3). DOI: 10.1088/1361-6404/ab531e.
22. Lomakin A.A. 1966. *Centrifugal and Axial Pumps*. Moscow-Leningrad: Mashinostroenie.
23. Pritchard P.J., J.W. Mitchell. 2015. *Fox and McDonald's Introduction to Fluid Mechanics*. 9th ed. John Wiley & Sons.
24. Crane Co. 1982. *Flow of Fluids through Valves, Fittings and Pipes*. Metric Edition-SI Units. Technical Paper No. 410M, Crane Co., New York.

Received 07.12.2025; accepted in revised form 23.04.2026